Cite this: CrystEngComm, 2012, DOI: 10.1039/C2CE25297J

http://pubs.rsc.org/en/content/articlelanding/2012/ce/c2ce25297j

ARTICLE TYPE

Characterization and humidity properties of $MgAl_2O_4$ powders Synthesized in a mixed salt composed of KOH and KCl

Bao-rang Li*; De-long Zhang; Nai-qiang Zhang;Jing-tao Li

Receivedxxxxx, *Acceptedxxxx*

In this paper, we have tried to prepare $MgAl_2O_4$ spinel by molten salt synthesis process using hydroxide as solvent. By controlling the amount of KCl in KOH, pure flower-like $MgAl_2O_4$ nanostructure could be synthesized at 1150°C. Powder X-ray diffraction, field emission scanning electron microscopy, and transmission electron microscopy were used to investigate structures and morphologies of the obtained products. The results showed that the 3D flower-like nanostructures are consisted of numerous 2D nano-flakes with the thickness of about several tens nano-meters. Further investigations on the possible formation mechanism revealed that a self-sacrificing template process was dominated for the formation of $MgAl_2O_4$ and the growth of the flower-like products was attributed to the competition between the growth rates along the directions perpendicular and parallel to the Al_2O_3 particles surfaces. Finally, an impedance-type humidity sensor was fabricated based on the flower-like $MgAl_2O_4$ nanostructure and tested with humidity performance providing that the as-prepared $MgAl_2O_4$ is suitable for high-performance humidity sensors.

Spinel oxides have the composition AB_2O_4, where A and B, for example, represent divalent and trivalent cations, respectively. Many spinels have important technical applications, for example, iron-containing spinels (ferrites) are important magnetic materials. Magnesium aluminate spinel ($MgAl_2O_4$) is one of the best known and widely used polycrystalline materials. It possesses a good combination of features such as high melting point, good mechanical strength, low dielectric constant and high resistance against both alkalis as well as acids. This makes it popular in many industrial applications, e.g., in chemistry, metallurgy and electronics. Recently, the developed $MgAl_2O_4$ sensing materials were found to be used for the application in typical operating conditions for PEM fuel cells [1].

The $MgAl_2O_4$ spinel is usually fabricated by the conventional method, wet chemical routes, molten salt synthesis (MSS), etc. [2-4]. MSS has many advantages such as cost effectiveness, easy setup, low temperature synthesis and controllable size of products. Therefore, the MSS process has been widely used for synthesis of single and multi-oxide powders [5]. Recently this process, a low-temperature technique, has been used to synthesize $MgAl_2O_4$. When the MSS is applied to prepare $MgAl_2O_4$, the used solvent is generally the basic chloride salts. Up to present, reports on using hydroxide as solvent are less found [6-14].

Due to its strong chemical activity, hydroxide can react with the used starting precursors and shift the equilibrium of the synthesis processes. For example, when $BaCO_3$ and TiO_2 were used as precursors to fabricate $BaTiO_3$, the synthesis temperature could be lowered to be 175°C for hydroxide salts while for chloride salts it was at least 700°C. In the case of chloride salts, the following reaction was obeyed, which was similar to that of the solid state reaction:

$$BaCO_3 + TiO_2 = BaTiO_3$$

However, under the case of hydroxide salts, the synthesis reaction could be modified as follow:

$$BaCO_3 + 2NaOH + TiO_2 = BaTiO_3 + Na_2CO_3 + H_2O$$

Obviously, this modification can enhance the diffusion process and shift the equilibrium of the synthesis processes resulting in an accelerated reaction dynamics. Similar results were also found by A.V. Gorokhovsky *et. al* [15]. In comparison with other salt solvents, hydroxide salt might have stronger influences on the products synthesis and characterization. So, using KOH as the flux, the MSS technique was applied to fabricate $MgAl_2O_4$ powders in the present work. By controlling the experimental conditions, flower-like $MgAl_2O_4$ powders composed of nano-flakes were synthesized successfully. Moreover, $MgAl_2O_4$ humidity sensor was fabricated and the as-prepared $MgAl_2O_4$ powders' humidity sensitivity property was characterized. To the best of our knowledge, the similar reports are not found in the opened literatures.

The reagents used in the experiment are all from Sinopharm Chemical Reagent CO. Ltd. MgO and Al_2O_3 were used as source materials for preparing $MgAl_2O_4$ sample using KOH as molten salt. An equi-molar composition of MgO and Al_2O_3 was homogeneously mixed by using ball mill, and followed by putting into an oven for drying. The dried power was later mixed with the salt and the salt/oxide weight ratios were designed to be 1:1, 2:1, 4:1, 6:1, 8:1 and 10:1, respectively. After being grinded for 2h using an agate mortar, the powder mixture was placed in an alumina crucible covered with an alumina lid, heated at different temperatures for 4h. When the crucible was cooled down to room temperature by furnace cooling, samples were collected and washed with deionized water to guarantee no ions left in the samples. Then the samples with deionized water were oven-dried before further characterization.

XRD patterns of the powder samples were recorded using a Rigaku Dmax-2500 automatic diffracto-meter equipped with Cu-Kα radiation (λ=0.15406nm). FE-SEM (JSM-7401F) was used to observe particle morphology. Prior to observation, the samples were dispersed in ethanol by ultrasonic processing, and then dropped on a clean silicon slice. The structure of the samples was further characterized by transmission electron microscope and high-resolution transmission electron microscope (HRTEM), which were performed on a JEOLJEM-2010 microscope at an accelerating voltage of 200 kV. Differential scanning calorimetry (DSC) measurements were made with the use of a liquid-nitrogen cooling accessory (DSC 404 F3 Pegasus). The specific surface area of the as-prepared powders was measured using the BET method (Micromeritics, ASAP 2010 N, USA).

In order to study its humidity sensing properties, the as-prepared powders were mixed with deionized water to form a paste. The paste was dip coated on a ceramic substrate (6 mm-3 mm, 0.5 mm thick) with five pairs of Ag–Pd interdigitated electrodes (electrodes width and distance: 0.15 mm) to form a sensing film dried in air at room temperature for 12 h. Finally, the humidity sensor was obtained after ageing at 95% relative humidity (RH) with a voltage of 1 V, 100 Hz for 24 h to improve stability and durability. Controlled humidity environments were obtained with saturated salt solutions in a closed glass vessel. The humidity sensitivity test was done by a ZL-5 intelligent LCR analyzer (made in Shanghai, China) at room temperature.

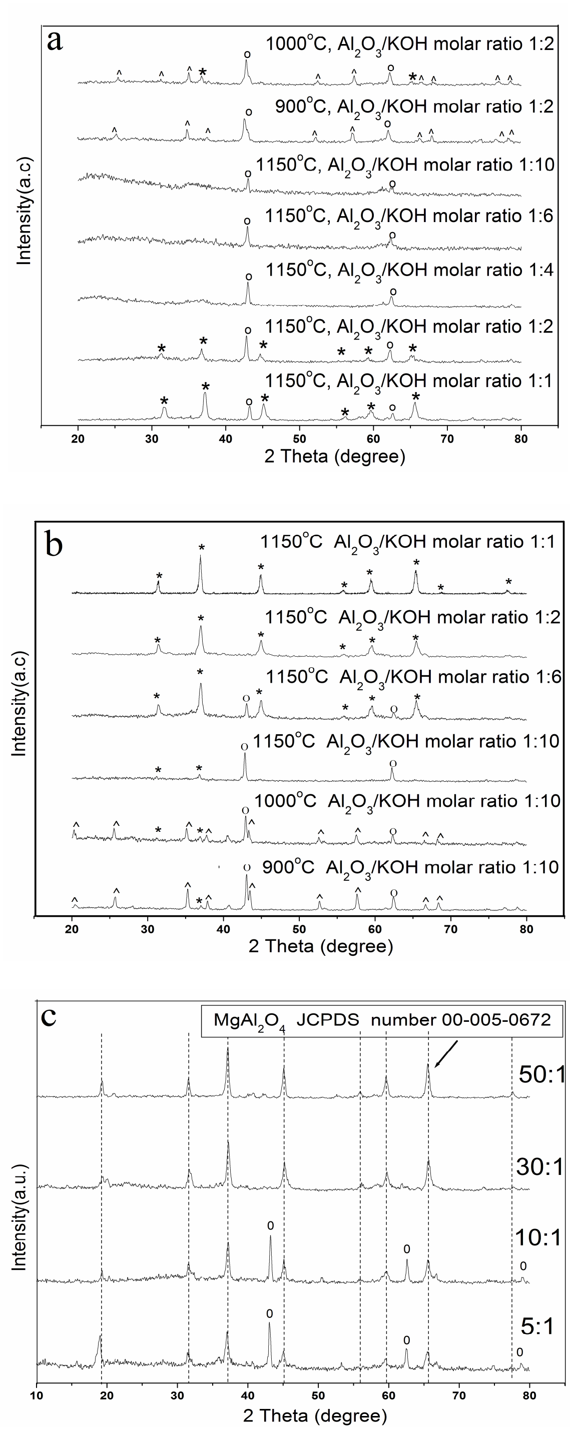

Fig.1 (a) XRD patterns of the products obtained by treatment of precursors for 4h at different temperatures ranging from 900 to 1150^{o}C in molten KOH salt. (b) XRD patterns of the products obtained by treatment of precursors for 4h at different temperatures ranging from 900 to 1150^{o}C in the mixed molten salt composed of KOH and KCl. The KCl /oxide weight ratio is 20:1; (c) XRD patterns of the samples with various KCl /oxide weight ratios. The Al_2O_3/ NaOH weight ratio is kept to be 1:2 while the KCl /oxide weight ratios were arranged from 5:1 to 50:1. Symbols *, O and ^ represent $MgAl_2O_4$, MgO and Al_2O_3 phase, respectively.

Fig. 1(a) shows XRD patterns of the samples calcined at different temperatures for 4h. The used salt is KOH and the molar ratios of Al_2O_3 and KOH are arranged from 1:2 to 1:10. The content of KOH has obvious influences on the formation of $MgAl_2O_4$. With the molar ratios higher than 1: 4, only the MgO peaks are found. $MgAl_2O_4$ phase can be observed as the molar ratios of Al_2O_3 and KOH are lower than 1: 4. Moreover, the amount of $MgAl_2O_4$ seems to increase with the molar ratios decreasing. When the molar ratio is lowered to be 1:1, the fraction of $MgAl_2O_4$ phase in the final product can increase to be nearly 80%.

For investigating the influences of the calcinations temperature on the formation of $MgAl_2O_4$, the sample with the molar ratio of 1: 2 is calcined at different temperatures and the corresponding XRD patterns are also displayed in Fig. 1(a). When the calcination temperatures are increased from 900 to 1150^{o}C, the fractions of $MgAl_2O_4$ phase in the products increase from 0% to 75%. This implies the stronger dependence of $MgAl_2O_4$ formation on the temperature. Moreover, Fig. 1(a) indicates that with single KOH as solvent, the synthesis temperature for pure $MgAl_2O_4$ is at least higher than 1200^{o}C, which show no advantages in comparison with other salt fluxes [6-7].

Fig.1（b）shows XRD patterns of the samples synthesized in a mixed salt composed of KOH and KCl. The molar ratios of Al_2O_3 and KOH are still in ranging from 1:2 to 1:10. The weight ratio of KCl and the starting materials is kept to be 20:1. Large amounts of $MgAl_2O_4$ are synthesized in samples when the molar ratios of Al_2O_3 and KOH are lower than 1: 6. Pure $MgAl_2O_4$ phase can be synthesized with the molar ratios of Al_2O_3 and KOH less than 1:2. However, when the molar ratios of Al_2O_3 to KOH are higher than 1: 6, the amounts of $MgAl_2O_4$ decrease significantly. For example, with increasing the molar ratios of Al_2O_3 to KOH from 6:1 to 10:1, the fractions of $MgAl_2O_4$ phase in the products tend to decrease significantly from 81% to 26%. This trend is very similar to that shown in Fig. 1(a). Therefore, Fig. 1(b) suggests the fixed amount of KCl is conductive to the formation of pure $MgAl_2O_4$ in the presence of KOH. Pure $MgAl_2O_4$ phase cannot be synthesized at relatively low temperatures in KOH when the oxides are used as precursors. In order to synthesize $MgAl_2O_4$, a proportional addition of KCl becomes necessary.

For investigating the possible effect of KCl amount on the formation of $MgAl_2O_4$, we make the following experiments. In our experiments, the molar ratio of Al_2O_3 and KOH is kept as 1:2. The weight ratios of KCl and the starting materials are designed to be arranged from 5:1 to 50:1. The calcinations temperature is still 1150^{o}C. Fig.1(c) shows the XRD patterns of the as-synthesized samples. As the weight ratios of KCl and the starting materials are lower than 10:1, the diffraction peaks of MgO can be observed, suggesting the amount of KCl might be an important factor for the formation of pure $MgAl_2O_4$.

In general, two mechanisms, ‘dissolution-precipitation’ and ‘template-formation’ are involved in MSS. With Al_2O_3 as template, the latter mechanism is reported to be dominated in MSS of $MgAl_2O_4$ [8]. According to this theory, molten salt synthesis procedure of $MgAl_2O_4$ should involve the following three steps. Firstly, the dissolved MgO (in the form of Mg^{2+}) diffuse onto Al_2O_3 particle surfaces and react in situ to synthesize

$MgAl_2O_4$. The reaction can be described as below:

$$Al_2O_3 + MgO = MgAl_2O_4 \quad (1)$$

Secondly, MgO further diffuse to the un-reacted Al_2O_3 core through the formed continuous $MgAl_2O_4$ spinel layer. Finally, the diffused MgO react with un-reacted Al_2O_3. Therefore, the synthesized spinel powder should retain the size and morphology of the Al_2O_3 when the single salt is used for preparing $MgAl_2O_4$. However, when KOH salts are used, some difference would happen due to its chemical activity. When KOH is added into the precursors, the following reactions would happen in the ball-milling process [16].

$$Al_2O_3 + 2KOH = 2KAlO_2 + H_2O$$

or

$$Al_2O_3+2KOH+3H_2O=2K[A(OH)_4] \quad (2)$$

$$MgO + H_2O = Mg(OH)_2 \quad (3)$$

Since potassium hydroxide were dissolved and well distributed in water, $KAlO_2$ could be produced due to the presence of reaction (2). With temperature increasing, water would evaporate and Al_2O_3 start to exist in the form of potassium meta-aluminate ($KAlO_2$) while magnesium hydroxide is reduced to magnesium oxide with no particles morphology transition. So, as the calcinations temperature is increased, $MgAl_2O_4$ can be synthesized via the following steps.

$$2K[Al(OH)_4] = 2KAlO_2 + 4H_2O \quad (4)$$

$$Mg(OH)_2 = MgO + H_2O \quad (5)$$

$$2KAlO_2 + MgO = K_2O + MgAl_2O_4 \quad (6)$$

Compared with reaction (1), the energy for triggering reaction（6）seems to be dependent upon the replacement of K^+ with Mg^{2+}, which suggested an ion-exchange approach based on molten-salt reaction for the synthesis of $MgAl_2O_4$. According to the reports of C.Y. Xu et al. [17], this synthesis process is named as a self-sacrificing template process. Due to the smaller ion radius of magnesium compared with potassium, the exchange of magnesium ion and potassium ion might occur during the molten-salt reaction, and finally $KAlO_2$ was totally changed into $MgAl_2O_4$. So, the formation process of $MgAl_2O_4$ in the case of KOH might be totally different from that in KCl.

When the molar ratios of Al_2O_3 and KOH are higher than 1: 2, according to the reaction equations (2) and (3), all the Al_2O_3 in the starting materials can react into $KAlO_2$. Since the newly formed $KAlO_2$ and MgO have low solubility in the residual KOH, they are enwrapped and separated by liquid KOH at high temperature, which would hinder mutual diffusion and further lead to a limit reaction between $KAlO_2$ and MgO. Obviously, such hindrance effect is connected closely with the content of KOH. The more the content of KOH is, the more remarkable the hindrance effect is. So, after calcination, no $MgAl_2O_4$ phase can be found in samples with the molar ratios of Al_2O_3 and KOH higher than 2: 1, as shown in Fig. 1(a). The final products should be a mixture of $KAlO_2$, KOH and MgO. After being washed and dried, only MgO and Al_2O_3 are left due to the following reactions:

$$KAlO_2 + 2H_2O = Al(OH)_3 + KOH \quad (7)$$

$$2Al(OH)_3 = Al_2O_3 + 3H_2O \quad (8)$$

When the molar ratios of Al_2O_3 to KOH is 1: 1, according to the reaction equations (2) and (3), all the KOH can be consumed due to its less dosage and its hindering effect would be weakened. Under these cases, both the newly formed $KAlO_2$ and left Al_2O_3 can react with MgO into $MgAl_2O_4$ by a process similar to the solid state reaction. So, $MgAl_2O_4$ phase can be found in the samples with the molar ratios of Al_2O_3 to KOH lower than 1: 2. However, in order to obtain pure $MgAl_2O_4$, a relatively higher temperature becomes necessary.

In the case of the KCl/KOH mixed salt, the molten KCl can weaken the hindrance effect produced by the liquid KOH. So, at high-temperature, magnesium oxide dissolved in KCl have opportunities to diffuse to the surface of potassium meta-aluminate ($KAlO_2$) or Al_2O_3 with the liquid KCl as carrier and there react for $MgAl_2O_4$. Obviously, this would be affected inevitably by the amounts of KCl due to the increased mount of salt can accelerate the dissolution and diffusion of magnesium oxide.

The TGA and DSC results of the material precursors before calcinations are shown in Fig. 2. At the first stage with temperature lower than 200°C, three small peaks of the thermal decomposition at 118, 156 and 170°C, respectively, can be found in the DSC curve. The corresponding mass loss value is less than 10%, which may be due to the removal of external water by surface tension and structure water by chemical bonds. At the second stage with temperature higher than 500°C, three typical peaks can be observed in DSC curve and the TGA curve shows a significant mass loss in the region of 700-1000°C. The peak around 627°C might be due to the phase transformation of potassium meta-aluminate [18]. The second peak around 758°C is obviously connected to the melt of potassium chloride (a little lower than the actual melting point of KCl , which is 770°C, due to the presence of KOH with a low melting point [19]) while the third peak around 825°C can be attributed to the formation of $MgAl_2O_4$ phase.

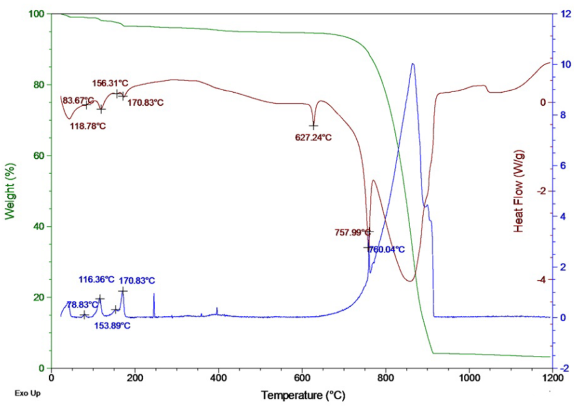

Fig. 2 DSC-TGA curve of the mixed starting materials heated to 1000 °C at a rate of 10 °C min^{-1}. The Al_2O_3/ NaOH weight ratio is kept to be 1:2 while the KCl /oxide weight ratios were 20:1.

Morphologies of the samples synthesized under various conditions were studies by SEM. Fig. 3(a) showed the sample synthesized in KOH were porous and comprised of wrinkle and self-assembled nano-flakes with the thickness of about 20 nm. Such characteristics were also reflected in the SEM image of sample synthesized in the mixed salt composed of KOH and KCl, as shown in Fig.3 (b). Large amounts of nano-flakes like $MgAl_2O_4$ radiating from and normal to the original large particles surfaces were produced. However, nano-flakes were not found in the sample synthesized in KCl. These observations suggested KOH can significantly change the particles morphology although it isn't conducive to the formation of $MgAl_2O_4$. With a combination of KOH and KCl, $MgAl_2O_4$ spheres composed of nano-flakes can be synthesized by MSS.

The effects of the amount of KCl on the $MgAl_2O_4$ particle morphology were also investigated. In this section, the KCl /oxide weight ratios were designed to be arranged from 5:1 to 50:1. Fig. 4(a) showed the SEM image of the samples synthesized with the KCl /oxide weight ratio as 5:1. Only a small quantity of the nano-flakes with scattered distribution was found on the large particles surfaces (circled parts in Fig. 4(a)). Large amounts of nano-flakes can be observed in samples with the KCl /oxide weight ratio as 10:1 and 30:1, respectively. The formed nano-flakes with uniform thickness agglomerated together and intercrossed with each other forming a porous structure (Fig. 4(b) and (c)), which exhibited a relatively large BET surface area of about 107.6 m^2/g (Fig. 4 (c)). Further increasing the ratios to 50:1, nano-flakes disappeared and the obtained particles morphology was very similar to that shown in Fig. 3(c), which indicated a stronger effect of potassium chloride on morphology in comparison with potassium hydroxide.

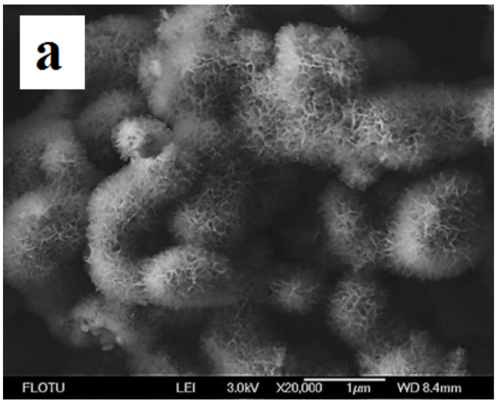

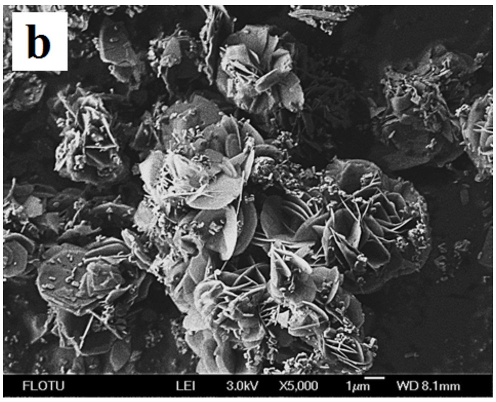

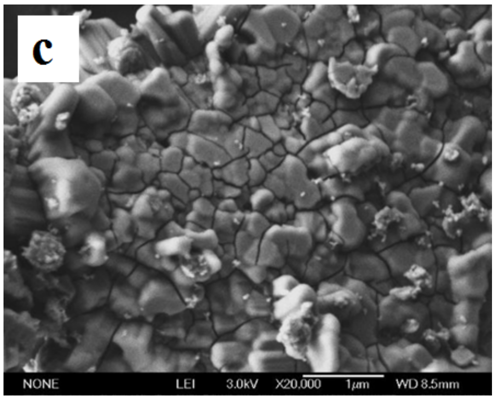

Fig.3 SEM images of the samples obtained under different conditions. The calcinations temperature is 1150°C. (a) KCl, the salt/oxide weight ratio is 20:1; (b) KCl &KOH, the Al_2O_3/ KOH weight ratio is 1:2, the KCl /oxide weight ratio is 20:1, the inset is the large magnification SEM images; (c) KOH, the Al_2O_3/ KOH weight ratio is 1:2;

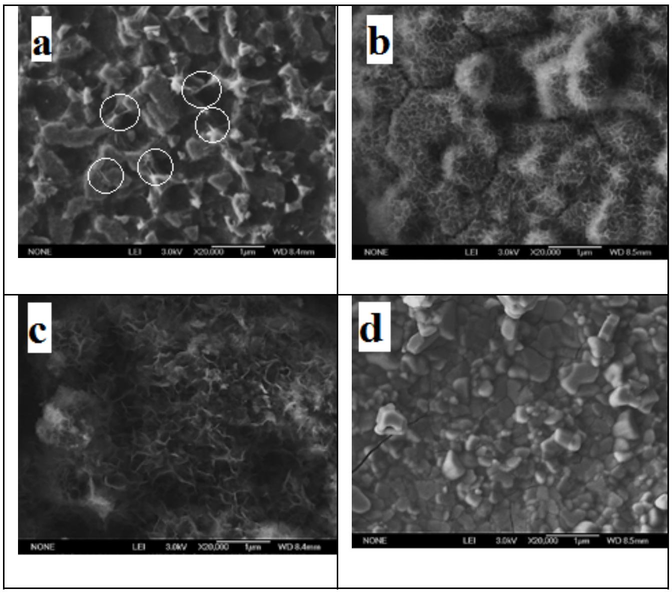

Fig.4 SEM images of the samples obtained under different conditions. The KCl /oxide weight ratios were arranged from 5:1 to 50:1.The Al_2O_3/ KOH weight ratio is kept to be 1:2. (a) 5:1; (b) 10:1; (c) 30:1; (d) 50:1.

To shed further light in the structural features, TEM analysis was carried out. A TEM image of the typical $MgAl_2O_4$ flakes is presented in Fig.5A, indicating that the dark area corresponds to the flake. The high magnification TEM image of the area selected by the circle in Fig.5A is given in Fig.5 B. The insets of Fig.5 B show a selected area electron diffraction pattern and HRTEM image taken from one of the flakes indicated by arrow, implying that the nano-flake is a good crystallinity with inter-planar spacing of about 0.23 nm, corresponding to the (222) plane of $MgAl_2O_4$.

On basis of the above experimental results, the possible formation mechanism of the flower-like structure can be proposed and is illustrated in Fig.6. Supposing the molten KCl can be mixed uniformly with KOH, MgO dissolved in KCl would have opportunities to precipitate forming $MgAl_2O_4$ (black point shown in Fig. 6) on the surface of the Al_2O_3 particles while no MgO can precipitate in the blank space occupied by KOH (shown in Fig. 6) since MgO isn't dissolved in KOH. So, at the initial stage, the formed $MgAl_2O_4$ would distribute sporadically on the surface of the Al_2O_3 particles. As the synthesis reactions go on, the formed $MgAl_2O_4$ would agglomerate into a net-like structure. As for the growth of the net-like structure, there are two possible growth directions: perpendicular or parallel to the Al_2O_3 particles surfaces, as shown in Fig. 6. The growth along the direction parallel to the Al_2O_3 particles surfaces is limited due to the lack of MgO in KOH while the direction perpendicular to the Al_2O_3 particles surfaces can have large growth rate due to the dissolved MgO in KCl. Moreover, the crystal growth perpendicular to the particles surfaces is squeezed inevitably by liquid KOH and preferentially grows along a certain direction to form 2D nano-flakes within proper reaction time. When many nano-flakes reach appropriate size and conglomerate, they usually tend to form sphere shapes to reduce the surface energy [20].

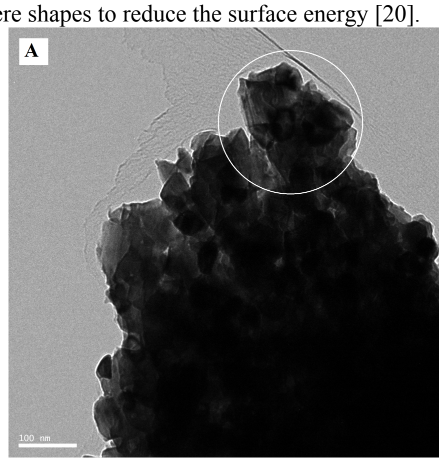

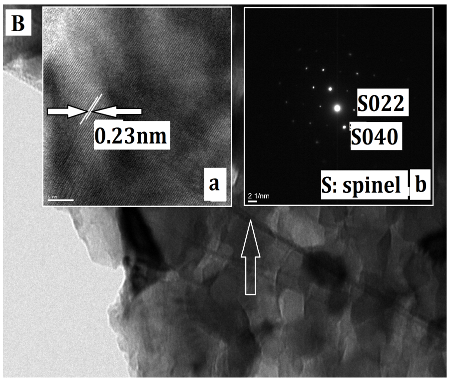

Fig.5 (A) TEM image of the flower-like products; (B) The enlarged TEM image of the part corresponding to the circled part in (A), Typical HRTEM image (b) and corresponding SAED pattern (a).

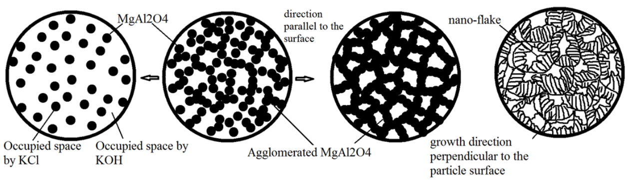

Fig.6 Scheme for the formation of the flower-like products

Our previous studies revealed that the 1V, 100 Hz AC signal is the best testing condition for inorganic material. Thus, we tested the humidity hysteresis phenomena for the sensor based on as-prepared $MgAl_2O_4$ by keeping the applied voltage at 1 V and the frequency at 100 Hz. Figure 7 shows the humidity hysteresis characteristic of the $MgAl_2O_4$-sensor by keeping the applied voltage at 1V and the frequency at 100 Hz. The solid lines stand for the course from low to high RH, corresponding to the absorption process, while the dash lines stand for the opposite direction, corresponding to the desorption process. Hysteresis is the time lag in the adsorption and desorption process, and is usually used to estimate the reliability of humidity sensors. As shown in Figure 7, it can be found from the plot, that the two lines almost overlapped when it is cycled back from high RH to low RH. This small hysteresis is essentially negligible and indicates a good reliability of the sensor. Figure 7(b) shows the response and recovery property of $MgAl_2O_4$ sensor by switching measurement atmosphere between 11% and 95% RH. The time required to achieve 90% of the total impedance change is defined as the response and recovery time. When RH increased from 11% to 95%, the response time is 10s, and the recovery time is 4s when RH decreased from 95% to 11%. These values further indicate $MgAl_2O_4$ sensor has a good response/recovery speed. Fig.7(c) gives the sensitivity repeatability of the sample. The $MgAl_2O_4$ materials show excellent repeatability of humidity sensitivity.

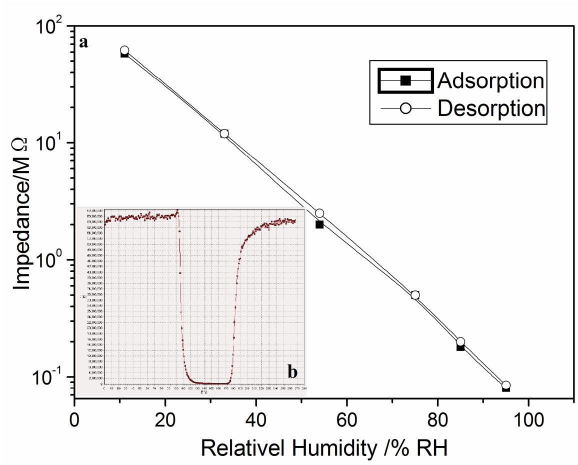

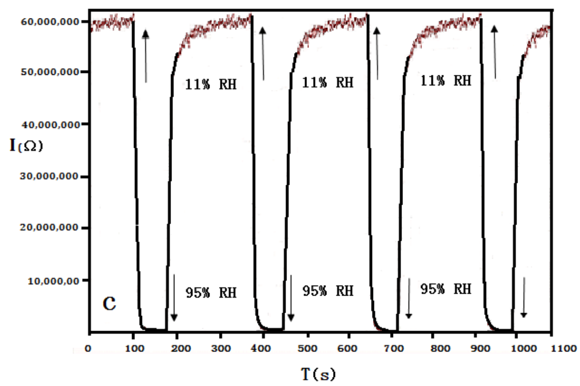

Fig.7 humidity properties of $MgAl_2O_4$ samples (a) Humidity hysteresis characteristic, the test condition was AC 1 V, 100 Hz; (b) Response and recovery property, the test condition was AC 1 V, 100 Hz. （c）the sensitivity repeatability of the sample

Conclusions

Using KCl/KOH as solvents, we have implemented a detailed study on MSS of $MgAl_2O_4$ with oxides as precursors. The results show pure $MgAl_2O_4$ cannot be synthesized with single KOH as solvent although KOH is found to have obvious effects upon the final particle morphology transition. In order to synthesize $MgAl_2O_4$, a mixed salt composed of KCl and KOH becomes necessary. Keeping the weight ratios of KCl and the starting materials higher than 10:1, pure $MgAl_2O_4$ spinel with flower-like nanostructure can be formed as the molar ratios of Al_2O_3 and KOH are lower than 1:2. Further investigations on the possible formation mechanism reveal that a self-sacrificing template process is dominated for the formation of $MgAl_2O_4$. Formation of the flower-like structure has close relations with the growth rates along the directions perpendicular or parallel to the Al_2O_3 particles surfaces. Finally, the humidity sensing property of the flower-like magnesium aluminate is investigated and the results confirm the as-prepared products is a promising high-performance humidity sensor candidate.

Acknowledgments

This work was supported by the funds from Beijing Natural Science Foundation of China（2152030）& National Natural Science Foundation of China (Grant No. 51471069).

Notes and references

Address: The National Thermal Power Engineering Technology Research Center & Key Laboratory of Condition Monitoring and Control or Power Plant Equipment, School of Energy, Power and mechanical Engineering, North China Electric Power University, Beijing 102206, P. R. China, Tel.: +86-010-6177-2355; Fax: +86-010-6177-2383;
Corresponding author: libr@ncepu.edu.cn

1. Z. W. Wang, C. L. Chang, X. S. Zhao, J. Power. Sources., 190 (2009)351-355 .
2. J. Chandradass, K. Hyeon Kim, J. Ceram. Proces. Res., 11(2010) 96-99.
3. P. Fu, W.Z. Lu, W. Lei, Mat. Res., 16 (2013)1516-1520.
4. I. Ganesh, Inter. Mater. Rev., 58 (2013) 63-112.
5. M. A. Einarsrud, T. Grande, Chem. Soc. Rev., 43(2014)2187-2190.
6. Y. Safaei-Naeini, M. Aminzare, F. Golestani-Fard, Ceram. Inter., 38(2012)841-845.
7. Y. Safaei-Naeini, F. Golestani-Fard, F. Khorasanizadeh, M. Aminzare, S. Zhang, Iranian. J. Mater. Sci. & Eng., 8(2011) 23-28.
8. D. D. Jayaseelan, S.W. Zhang, S. Hashimoto, W. Edward Lee, J. Eur. Ceram. Soc., 27(2007)4745-4749.
9. Y. Zhang, R.Y. Li, X.R. Zhou, M. Cai, X.L. Sun, J. Phys. Chem. C., 112(2008)10038-10042.
10. E. K. Omid, R. Naghizadeh, H. R. Rezaie, J. Ceram. Pro. Res., 14 (2013) 445-447.
11. S.W. Zhang, D. D. Jayaseelan, G. Bhattacharya, W. E. Lee, J. Am. Ceram. Soc., 89(2006)1724-1726.
12. J. Zhang, D.H. Li, Y.C. Zhou, J. Am. Ceram. Soc., 92 [5] (2009) 1074-1078.
13. R. Fazlia, M. Fazli, Y. Safaei-Naeini, F. Golestani-fard, Ceram. Inter., 39(2013)6265-6270.
14. M. Salavati-Niasari, M. R. Loghman-Estarki, F. Davar. Synthesis, Inorg. Chim. Acta, 362 (2009) 3677-3681.
15. A.V Gorokhovsky, J.I Escalante-Garcia, T Sánches-Monjarás, G Vargas-Gutierrez, Mater. Lett., 58(2004)2227-2230.
16.Chunhua Du, Shili Zheng, Yi Zhang, Fluid Phase Equilibria, 238 (2005) 239–241.
17. C.Y. Xu, L. Zhen, R. Yang, Z. L. Wang, J. AM. CHEM. SOC., 129 (2007) 15444-15445.
18. Arnoud P. de Kroon, Gu¨nter W. Scha¨fer, Fritz Aldinger, J. Alloy. Compd., 314 (2001) 147–153.
19. Hui-Ling Li, Zhen-Ni Du, Gen-Lin Wang, Yong-Cai Zhang, Mater. Lett., 64(2010) 431–434.
20. Jinhui Jiang , Weidong Shi , Shuyan Song , Qingli Hao, et al., J. Power. Sources., 248 (2014) 1281-1289.